Transient Heat Transfer Analysis of Housing and PMM Using 3–D FE Code

Themistoklis D. Kefalas, *Member, IEEE*, and Antonios G. Kladas, *Senior Member, IEEE*

***Abstract* -- This paper proposes finite element (FE) numerical methodologies for the transient heat transfer analysis of highly integrated actuators for demanding aerospace applications. A FE surface heat source is developed which permits to independently simulate the thermal performance of the housing of the actuator. As a result, the complexity of the FE model is reduced significantly and the computational cost is minimized. The proposed technique is integrated into a three dimensional (3–D) FE package that employs preprocessors capable of producing highly parameterized cooling housings of arbitrary configurations. The specific 3–D FE code was used for the transient heat transfer analysis of a surface mounted permanent magnet motor (PMM) and its non–standardized and unsymmetrical cooling housing.**

***Index Terms*--Actuators, aerospace engineering, aerospace industry, computer aided analysis, electric machines, finite element methods, numerical analysis, permanent magnet machines, thermal analysis, time domain analysis.**

I. Nomenclature

$[\mathbf{K}]$	Conductance matrix of a FE element (4×4).
$[\mathbf{C}]$	Heat storage matrix of a FE element (4×4).
$[\mathbf{T}]$	Temperature vector of a FE element (4×1).
$[\mathbf{F}]$	Thermal load vector of a FE element (4×1).
P_{Losses}	Total losses of the motor (W).
$A_{Contact}$	Housing area in contact with the motor (m^2).
$A_{facet}^{(e)}$	Area of a facet of a tetrahedral element (m^2).
FPCW	Full pitch concentrated winding.
FSCW	Fractional slot concentrated winding.
FSCW1	Non–overlapping, all–teeth–wound FSCW.
FSCW2	Non–overlapping, alternate–teeth–wound FSCW.

II. Introduction

THE PRESENT paper deals with methods for the thermal performance evaluation of highly integrated permanent magnet motors (PMM) used in challenging thermodynamic environments encountered in aerospace actuation applications. Such actuators make use of non–standardized, unsymmetrical cooling housings of complex geometry that in most cases are totally enclosed natural convection (TENV) type. Engineers are forced to adopt such unconventional solutions due to current political, economical, and environmental trends that lead to the all electric aircraft (AEA) concept and to the corresponding elimination of hydraulic power sources [1], [2]. Due to the absence of hydraulic fluid, heat will not be dissipated from electric actuators used in demanding aerospace applications [3], [4]. As a result, such actuators work under severe thermodynamic environments in confined spaces [5], where localized heat effects and the absence of forced cooling affect the motor performance and particularly permanent magnet characteristics [6], [7].

In the aforementioned cases the solution of the thermal problem requires detailed three dimensional (3–D) finite element (FE) unsteady heat transfer analysis. The full 3–D modeling is required because the cooling housing usually has no two dimensional (2–D) or 3–D symmetry. Also, the conventional approach for electric machine thermal analysis, which is based on lumped–parameter networks [8]–[18], presents disadvantages comparing to the FE method as the former does not permit detailed temperature gradient calculation in complex geometries.

Moreover, the computational fluid dynamic (CFD) analysis [19]–[24], is not suitable in the specific cases since it requires substantial computational resources and the convective heat transfer mechanism is insignificant due to the absence of forced cooling conditions.

In order to reduce the computational effort of the thermal analysis and to simplify the construction of the FE model of such actuators, it is proposed to use a surface heat source which allows simulating the cooling housing independently from the PMM. The specific method is integrated to a 3–D FE code assembled by the authors that includes preprocessors capable of modeling cooling housings of arbitrary configurations.

III. 3–D FE Code and Related Techniques

A. Surface Heat Source of the Cooling Housing

The 3–D FE unsteady heat transfer analysis of the cooling housing is carried out independently from the analysis of the motor by making use of a surface heat source. The specific surface heat source is applied to the area of the cooling housing in thermal contact with the electric machine.

The FE formulation of the surface heat source is based on the following procedure in the case of first order tetrahedral elements. Initially, the equations for a single element are formed (1), where $[\mathbf{K}]$ is the (4×4) conductance matrix,

The research leading to these results has received funding from the European Union Seventh Framework Programme (FP7/2007–2013) under grant agreement AAT.2008.4.2.4–234119 CREAM within TEIP Consortium Member.

T. D. Kefalas is with the School of Electrical and Computer Engineering, National Technical University of Athens, 15780 Athens, Greece (e–mail: thkefala@central.ntua.gr).

A. G. Kladas is with the School of Electrical and Computer Engineering, National Technical University of Athens, 15780 Athens, Greece (e–mail: kladasel@central.ntua.gr).

978-1-5090-2538-1/16/$31.00 ©2016 IEEE

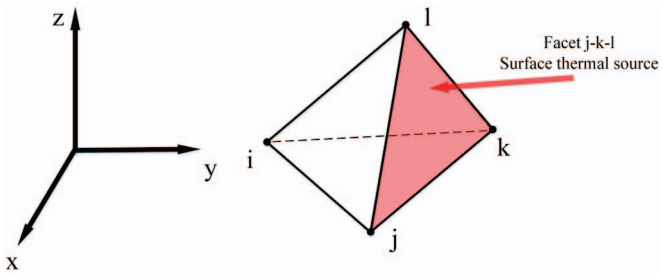

Fig. 1. Application of the surface thermal source to a tetrahedral element.

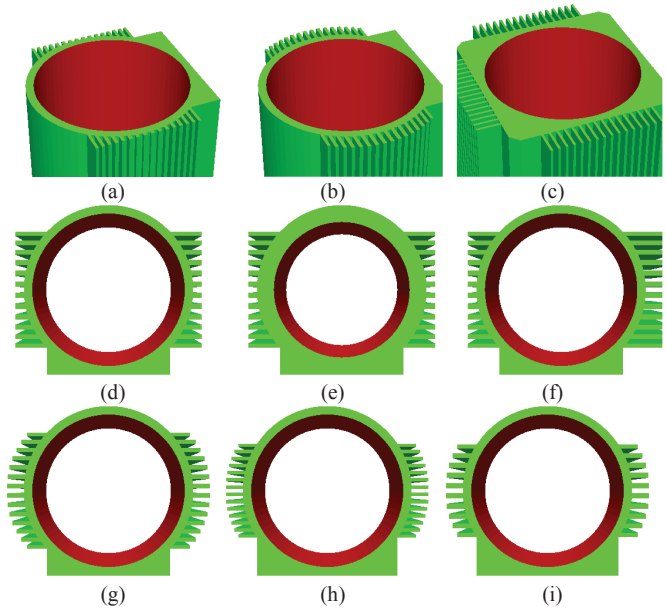

Fig. 2. (a), (b), and (c) Three non–standardized housing types. (d) Front view of 1st housing type. (e) Reduction of housing inner radius. (f) Increase of width of right fins. (g) Front view of 2nd housing type. (h) Reduction of aperture of fins. (i) Reduction of number of fins.

$[\mathbf{C}]$ is the (4×4) heat storage matrix, $[\mathbf{T}]$ is the (4×1) temperature vector, and $[\mathbf{F}]$ is the (4×1) thermal load vector.

$$([\mathbf{K}]+[\mathbf{C}])\cdot[\mathbf{T}]=[\mathbf{F}] \tag{1}$$

Then the attributes of the three nodes of each of the four facets of the tetrahedral element are verified. In the case where all nodes of a facet have the same attribute that correspond to the surface heat source e.g., nodes $j-k-l$ shown in Fig. 1, then the thermal load vector is updated as follows:

$$\begin{bmatrix} F_i' \\ F_j' \\ F_k' \\ F_l' \end{bmatrix} = \begin{bmatrix} F_i \\ F_j \\ F_k \\ F_l \end{bmatrix} + \frac{P_{Losses}}{A_{Contact}} \cdot \frac{A_{facet}^{(e)}}{3} \cdot \begin{bmatrix} 0 \\ 1 \\ 1 \\ 1 \end{bmatrix} \tag{2}$$

where P_{Losses} are the total losses of the electric machine,

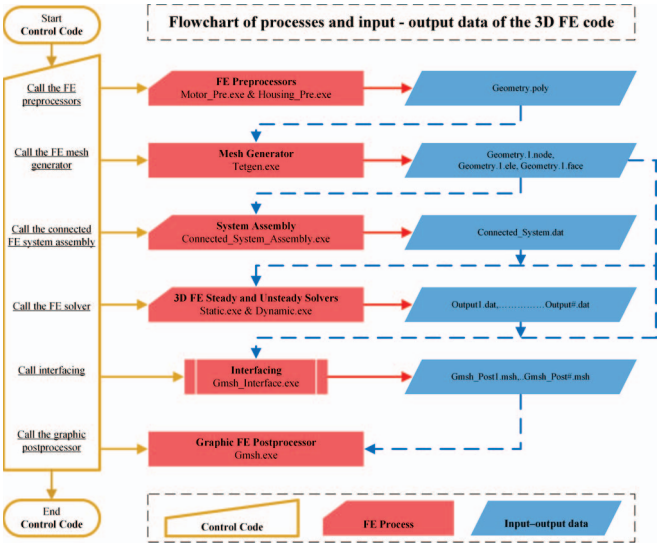

Fig. 3. Flowchart of the FE processes and input – output data of the 3–D FE thermal code.

$A_{Contact}$ is the area of the housing in thermal contact with the electric machine, and $A_{facet}^{(e)}$ is the area of the $j-k-l$ facet of the tetrahedral element e.

B. PMM and Cooling Housing 3–D FE Preprocessors

The authors utilized a FE preprocessor that enables the generation of an arbitrary number of 3–D cooling housing configurations, including standardized and non–standardized housings. The specific preprocessors parameterize a large number of variables such as the number of fins, ratio of fin spacing to fin thickness, unsymmetrical fin width, axial length, etc. The aforementioned is demonstrated in Fig. 2, where the preprocessor was used for the generation of three unconventional cooling housings and then for the modification of some of their variables.

Accordingly, another preprocessor is employed for the generation of the FE model of the PMM that also parameterizes a very large number of variables and three different windings types, full pitch concentrated winding (FPCW), non–overlapping, all–teeth–wound, fractional slot concentrated winding (FSCW1), and non–overlapping, alternate–teeth–wound, fractional slot concentrated winding (FSCW2). The preprocessors are also used for the application of identifiers, representing material properties, boundary conditions and loads, to the volumes and surfaces of the FE models.

C. Description of the Processes of the 3–D FE code

The 3–D FE code consists of several processes that read input files and produce output files of appropriate format. The flow of the FE code is managed by a control code that calls and passes variables to the rest of the processes. The surface heat source technique is integrated in the FE heat transfer solvers. Fig. 3 shows a flowchart of the processes, input files, and output files of the 3–D FE code. The description of the individual processes follows in the next six paragraphs.

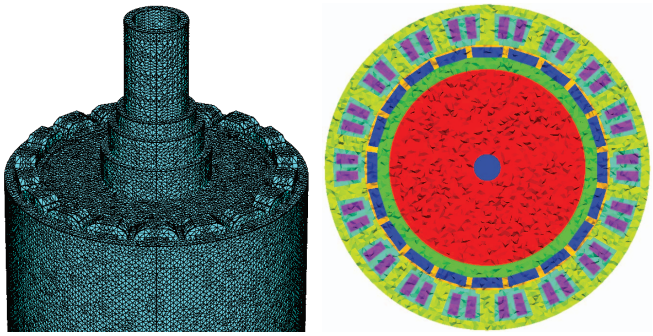

(a) (b)

Fig. 4. Surface mounted PMM. (a) Detail of the FE mesh. (b) Cross–section showing different regions of the FE model.

TABLE I
GEOMETRIC AND OPERATIONAL PARAMETERS OF THE PMM

Parameter	Value
Number of phases	3
Number of poles	20
Number of stator slots	18
Motor active length (mm)	120
Shaft radius (mm)	29
Rotor inner radius (mm)	32.75
Rotor outer radius (mm)	35.75
Magnet angle (degrees)	15.3
Gap width (mm)	0.5
Stator inner radius (mm)	36.25
Stator outer radius (mm)	48

1) Control Code: The control code calls the FE preprocessors which generate the FE geometries of the PMM and the housing, and then assign identifiers to the volumes and to the surfaces of the 3–D models.

2) Mesh Generation: The mesh generator is called, and the control program passes to it values that define the size and quality of the mesh. The input for the mesh generator is a file with extension *.poly produced by the preprocessors.

3) Connected System Assembly: The FE system assembly code is called. The input of this code are files with extensions *.ele and *.node, produced by the mesh generator code. These two files contain lists of the nodes of each tetrahedral element and the Cartesian coordinates of each node of the mesh respectively. The specific code incorporates a modified Morse technique [3], [4].

4) Unsteady Heat Transfer Solver: The 3–D FE unsteady solver is called. The input of this code are the two files with extensions *.ele and *.node, and the file with extension *.dat generated by the FE system assembly code. A file with extension *.dat is generated for every time–step of the unsteady analysis as shown in Fig. 3. In this stage of the analysis, material attributes, boundary conditions, and loads are assigned to the FE model and the storage of the stiffness matrix is carried out.

5) Interfacing: A sub–process is called that reads the file with extension *.face produced by the mesh generator and the solution files of the FE solver and produces the same number of files with extension *.msh.

6) Postprocessing: The postprocessor is called that reads the file with extension *.msh produced by the interfacing sub–process and generates graphical representations of the temperature distribution of the 3–D models.

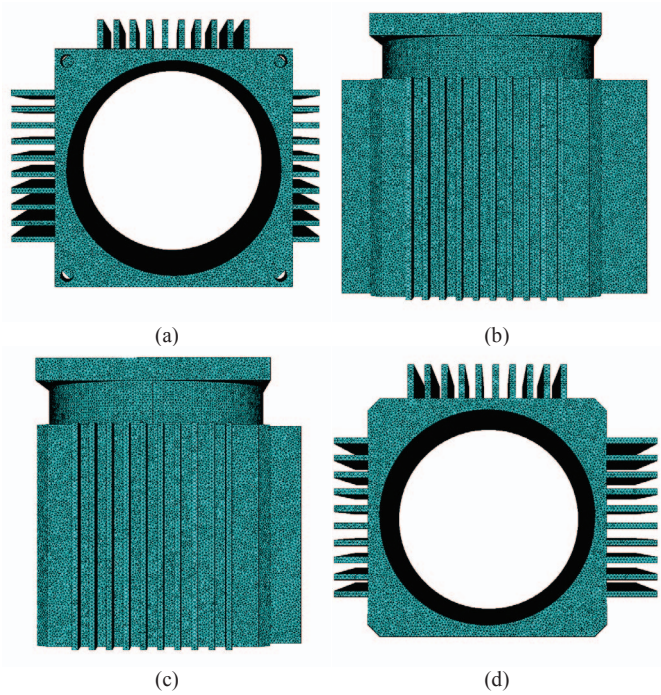

(a) (b) (c) (d)

Fig. 5. 3–D FE mesh of the cooling housing. (a) Front view. (b) Top view. (c) Side view. (d) Back view.

TABLE II
GEOMETRIC PARAMETERS AND MATERIAL PROPERTIES OF THE COOLING HOUSING

Parameter	Value
Number of fins	30
Fin spacing to fin thickness ratio	2
Front plate axial length (mm)	10
Axial length of cylinder (mm)	20
Axial length of fins (mm)	100
Housing inner radius (mm)	48
Housing outer radius (mm)	53
Width of right fins (mm)	15
Width of top fins (mm)	15
Width of left fins (mm)	22.5
Thermal conductivity ($W \cdot m^{-1} \cdot K^{-1}$)	14.425
Specific heat capacity ($J \cdot K^{-1} \cdot m^{-3}$)	$3.984 \cdot 10^6$

For the mesh generation and the graphics postprocessing the open access codes TetGen, TetView, and Gmsh were used [25], [26]. The rest of the processes were written by the authors using Visual Fortran and Visual Basic.

IV. HOUSING AND PMM DESCRIPTION

A. Surface Mounted PMM

A surface mounted PMM was designed and optimized for extremely high ambient temperature environmental conditions encountered in an aerospace application. Table I shows the design parameters of the PMM as obtained by a Rosenbrock based optimization algorithm [27], and Fig. 4 shows the respective geometry and FE mesh. High temperature, samarium cobalt (SmCo), permanent magnets and a FSCW1 configuration were used for the specific machine. The proposed PMM topology presents maximum torque per copper loss square root ratio, minimum torque ripple, and minimum back–EMF harmonic content

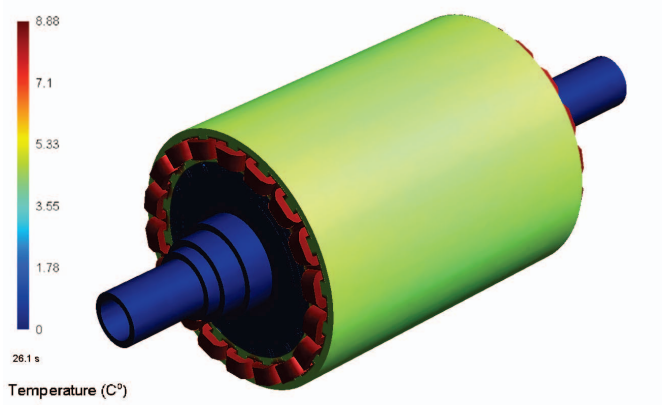

(a)

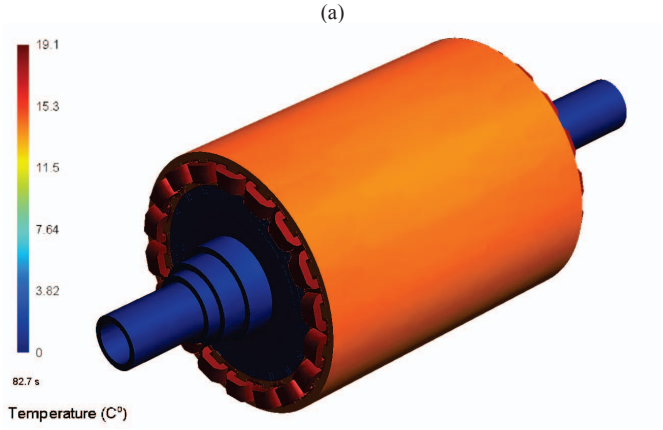

(b)

Fig. 6. Temperature distribution of the PMM obtained at 1200 r/min, with phase currents of 9.759 A. (a) 26.1 s. (b) 82.7 s.

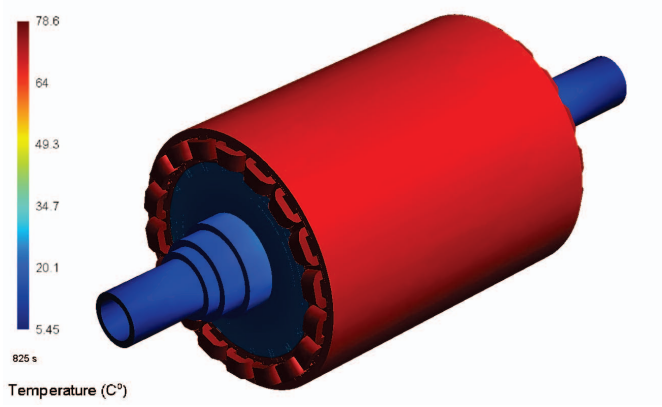

(a)

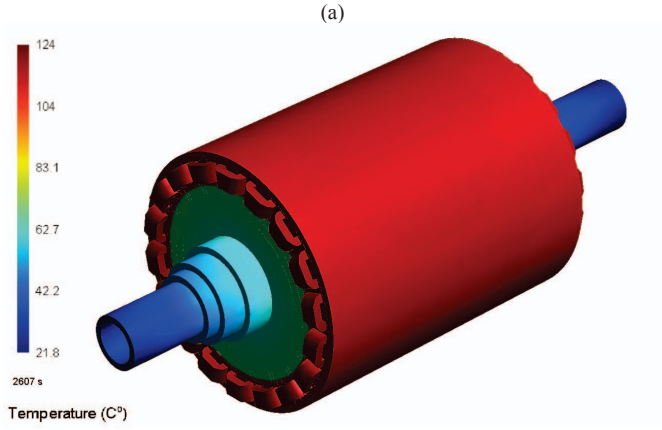

(b)

Fig. 7. Temperature distribution of the PMM obtained at 1200 r/min, with phase currents of 9.759 A. (a) 825 s. (b) 2607 s.

comparing to FPCW, and FSCW2 configurations [27]. A number of PMM prototypes were used for temperature measurements in order to validate the FE code of Section III.

B. Cooling Housing

The parameters of the cooling housing under consideration are shown in Table II. Also, Fig. 5 shows the FE mesh and the geometry of the cooling housing.

The housing configuration was selected so that there is no 2–D or 3–D symmetry. For instance the right fins are shorter than the left fins, and one–sixth of the axial length of the PMM is in thermal contact with the front cylinder and the rest five–sixths of the axial length of the PMM are in thermal contact with the housing fins. Consequently, it is not possible to use a 2–D FE model or use one–quarter or one–half of the 3–D model. This in turn leads to a large FE mesh and an increased computational cost.

Such non–standardized, unsymmetrical, TENV type, cooling housings tend to occur more and more often in contemporary aerospace actuation applications [4], in contrast with water jacket configurations used in vehicle powertrain applications [28], [29].

V. 3–D FE Unsteady Heat Transfer Analysis

A number of unsteady heat transfer analyses of the PMM and the cooling housing were carried out using the FE code of Section III. In both cases the optimum mesh size was determined by a sensitivity analysis. The large number of the analyses was tackled by using four conventional personal computers with a total of nine CPUs, and appropriate scheduling.

Every analysis, either an unsteady heat transfer solution or an assembly of the FE connected system, is a single–threaded application that consumes 100 % of the computational resources of a single CPU. Thus, by assigning a different analysis to each CPU it was possible to solve at the same time nine different problems of the FE models of the PMM and the cooling housing.

A. PMM Temperature Distribution

Winding and iron losses distribution of the PMM i.e., P_{Losses} where determined by static 2–D FE electromagnetic analyses [30]–[33]. The temperature dependent demagnetization characteristics of the SmCo permanent magnets of the PMM were taken into consideration by using a set of demagnetization curves for various ambient temperatures and an appropriate interpolation scheme.

Figs. 6, 7 show the temperature distribution of the PMM for four time–steps of the unsteady heat transfer analysis. The FE mesh size used for the specific analysis is equal to $4.0 \cdot 10^6$ elements. The results were obtained by a 10–step analysis. The duration of each time–step was determined by a time–step generator that enables the improvement of the resolution during the initial steps of the unsteady analysis, the minimization of the required steps, and the reduction of the computational cost of the unsteady analysis.

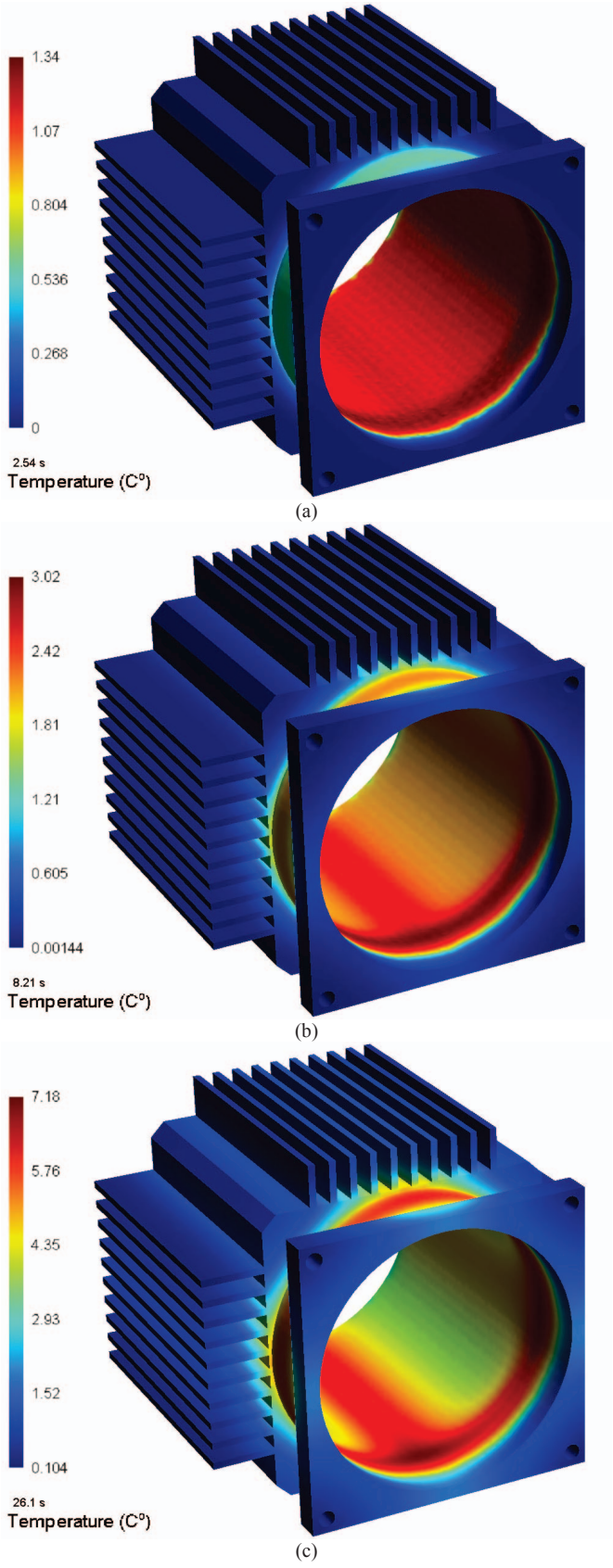

Fig. 8. Temperature distribution of the housing. Analysis was carried out for $A_{Contact} \approx 0.0362$ m^2 and $P_{Losses} = 200$ W. (a) 2.54 s. (b) 8.21 s. (c) 26.1 s.

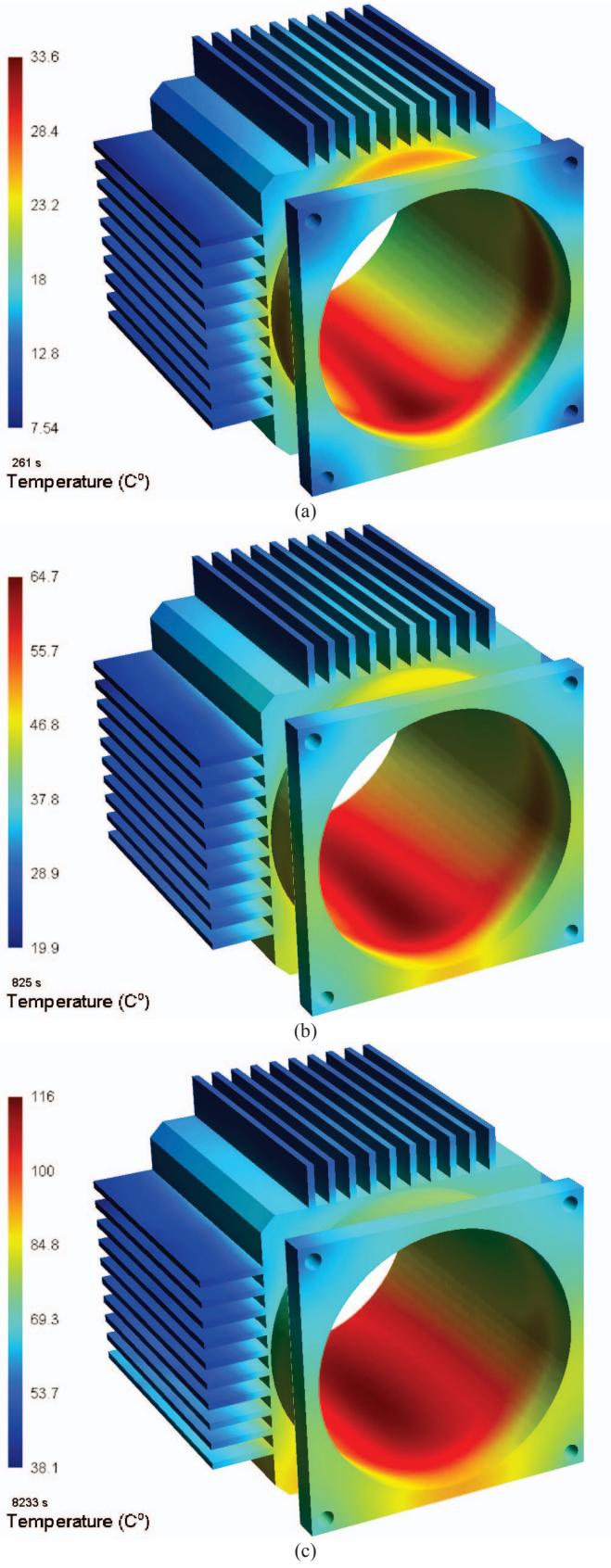

Fig. 9. Temperature distribution of the housing. Analysis was carried out for $A_{Contact} \approx 0.0362$ m^2 and $P_{Losses} = 200$ W. (a) 261 s. (b) 825 s. (c) 8233 s.

B. Housing Temperature Distribution

The thermal loading of the cooling housing was carried out by applying in the inner area of the housing, in thermal contact with the PMM, the surface heat source of Section III.A. Figs. 8, 9 show the temperature distribution of the cooling housing for six time–steps of the unsteady analysis.

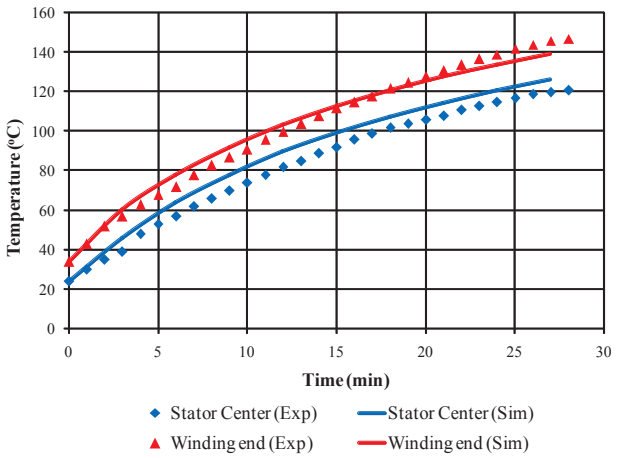

Fig. 10. Comparison of simulated versus measured temperature variation of the PMM (stator and winding end).

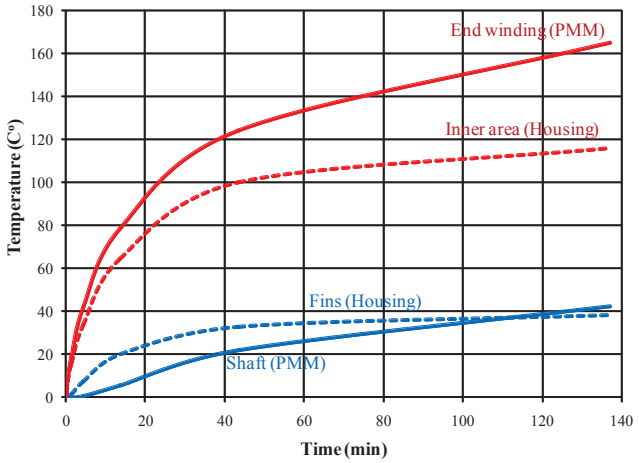

Fig. 11. Local maximum and local minimum temperature rise variation of the PMM and cooling housing over 140 min.

Analysis time ranges from 0.18 s to 8,233 s and the time–step ranges from 0.18 s for the first step to 5,626 s for the last step. The FE mesh size used for the specific analysis is equal to $4.55 \cdot 10^6$ elements.

It can be seen from Figs. 8, 9 that the heat is transferred gradually from the inner area in contact with the PMM to the rest of the housing. Also, the cylinder behind the front plate, which is in thermal contact with one–sixth of the PMM, has a distinctively larger temperature than the rest of the cooling housing.

C. *Experimental Verification*

The FE code was validated by temperature measurements carried out under various load conditions of the PMM. A data acquisition (DAQ) system, a torque gauge, variable electrical loads, and type–k thermocouples were used for the temperature measurements.

Fig. 10 shows a comparison of the 3–D FE simulated and measured temperature variation for two locations of the PMM i.e., the stator and the winding end. The specific measurements were carried out at constant phase currents of 9.25 A, at 1,200 r/min for 28 min, and for an ambient temperature of 25 °C. Simulated and measured temperature variation agrees within 1% to 4% in both cases.

Fig. 11 shows the corresponding local maximum and local minimum temperature rise variation of the PMM and the cooling housing as obtained by the unsteady heat transfer analysis. The specific analysis was carried out for constant phase currents of 9.759 A, and for a simulated time period of approximately 137 min. For the application of the surface heat source to the area of the cooling housing in thermal contact with the PMM, the corresponding P_{Losses} was equal to 200 W.

According to Fig. 11, the time constant is approximately 30 min. Also, Fig. 11 shows clearly that the winding end of the PMM is the critical temperature component of the actuator and that heat is also removed from the shaft and the rotor.

VI. Conclusion

High efficiency actuators for demanding aerospace applications are complex devices that work under short overload conditions and harsh environmental conditions. In order to accurately predict the thermal performance of such devices a detailed 3–D representation and an unsteady heat transfer analysis is needed.

The setup of the respective models and the analysis of such actuators can be simplified by modeling the cooling housing independently from the electric machine. This is achieved by using a surface heat source that is applied to the area of the cooling housing in thermal contact with the electric machine.

Furthermore, the paper proposes FE preprocessors that can generate cooling housings of arbitrary configurations. The aforementioned is important as non–standardized housing configurations are becoming more and more common in cases of highly integrated actuators installed in confined spaces.

Finally, the developed FE code has task parallelism computing capabilities i.e., a desktop computer with a quad–core processor is capable of executing simultaneously four threads of the FE code. As a result, the specific 3–D FE code is useful for sensitivity analysis and for integration to an optimization process.

VII. References

[1] W. Cao, B. C. Mecrow, G. J. Atkinson, J. W. Bennett, and D. J. Atkinson, "Overview of electric motor technologies used for more electric aircraft (MEA)," *IEEE Trans. Ind. Electron.*, vol. 59, no 9, pp. 3523–3531, Sep. 2012.

[2] X. Huang, A. Goodman, C. Gerada, Y. Fang, and Q. Lu, "Design of a five–phase brushless DC motor for a safety critical aerospace application," *IEEE Trans. Ind. Electron.*, vol. 59, no 9, pp. 3532–3541, Sep. 2012.

[3] T. D. Kefalas and A. G. Kladas, "Finite element transient thermal analysis of PMSM for aerospace applications," in *Proc. ICEM*, 2012, pp. 2566–2572.

[4] T. D. Kefalas and A. G. Kladas, "Thermal investigation of permanent–magnet synchronous motor for aerospace applications," *IEEE Trans. Ind. Electron.*, vol. 61, no 8, pp. 4404–4411, Aug. 2014.

[5] Z. Xu, C. Tighe, M. Galea, T. Hamiti, C. Gerada and S. J. Pickering, "Thermal design of a permanent magnetic motor for direct drive wheel actuator," in *Proc. ICEM*, 2014, pp. 2186–2192.
[6] M. Beniakar, T. Kefalas, and A. Kladas, "Investigation of the impact of the operational temperature on the performance of a surface permanent magnet motor," *Journal of Materials Science Forum*, vol. 670, pp. 259–264, 2011.
[7] J. Pyrhönen, S. Ruoho, J. Nerg, M. Paju, S. Tuominen, H. Kankaanpää, R. Stern, A. Boglietti, and N. Uzhegov, "Hysteresis losses in sintered NdFeB permanent magnets in rotating electrical machines," *IEEE Trans. Ind. Electron.*, vol. 62, no. 2, pp. 857–865, Feb. 2015.
[8] D. G. Dorrell, "Combined thermal and electromagnetic analysis of permanent–magnet and induction machines to aid calculation," *IEEE Trans. Ind. Electron.*, vol. 55, no 10, pp. 3566–3574, Oct. 2008.
[9] J. Nerg, M. Rilla, and J. Pyrhönen, "Thermal analysis of radial–flux electrical machines with a high power density," *IEEE Trans. Ind. Electron.*, vol. 55, no 10, pp. 3543–3554, Oct. 2008.
[10] A. Di Gerlando, G. Foglia, and R. Perini, "Permanent magnet machines for modulated damping of seismic vibrations: Electrical and thermal modeling," *IEEE Trans. Ind. Electron.*, vol. 55, no 10, pp. 3602–3610, Oct. 2008.
[11] N. Jaljal, J.–F. Trigeol, and P. Lagonotte, "Reduced thermal model of an induction machine for real–time thermal monitoring," *IEEE Trans. Ind. Electron.*, vol. 55, no 10, pp. 3535–3542, Oct. 2008.
[12] Z. Gao, R. S. Colby, T. G. Habetler, and R. G. Harley, "A model reduction perspective on thermal models for induction machine overload relays," *IEEE Trans. Ind. Electron.*, vol. 55, no 10, pp. 3525–3534, Oct. 2008.
[13] C. Kral, A. Haumer, and T. Bäuml, "Thermal model and behavior of a totally–enclosed–water–cooled squirrel–cage induction machine for traction applications," *IEEE Trans. Ind. Electron.*, vol. 55, no 10, pp. 3555–3565, Oct. 2008.
[14] G. Traxler–Samek, R. Zickermann, and A. Schwery, "Cooling airflow, losses, and temperatures in large air–cooled synchronous machines," *IEEE Trans. Ind. Electron.*, vol. 57, no 1, pp. 172–180, Jan. 2010.
[15] N. Bracikowski, M. Hecquet, P. Brochet, and S. V. Shirinskii, "Multiphysics modeling of a permanent magnet synchronous machine by using lumped models," *IEEE Trans. Ind. Electron.*, vol. 59, no 6, pp. 2426–2437, Jun. 2012.
[16] J. Le Besnerais, A. Fasquelle, M. Hecquet, J. Pellé, V. Lanfranchi, S. Harmand, P. Brochet, and A. Randria, "Multiphysics modeling: Electro–vibro–acoustics and heat transfer of PWM–fed induction machines," *IEEE Trans. Ind. Electron.*, vol. 57, no 4, pp. 1279–1287, Apr. 2010.
[17] K. Dimolikas, T. D. Kefalas, P. Karaisas, Z. K. Papazacharopoulos, and A. G. Kladas, "Lumped–parameter network thermal analysis of permanent magnet synchronous motor," *Journal of Materials Science Forum*, vol. 792, pp. 233–238, 2014.
[18] T. D. Kefalas and A. G. Kladas, "3–D FEM and lumped–parameter network transient thermal analysis of induction and permanent magnet motors for aerospace applications," *Journal of Materials Science Forum*, vol. 856, pp. 245–250, 2016.
[19] F. Marignetti, V. D. Colli, and Y. Coia, "Design of axial flux PM synchronous machines through 3–D coupled electromagnetic thermal and fluid–dynamical finite–element analysis," *IEEE Trans. Ind. Electron.*, vol. 55, no 10, pp. 3591–3601, Oct. 2008.
[20] C. Micallef, S. J. Pickering, K. A. Simmons, and K. J. Bradley, "Improved cooling in the end region of a strip–wound totally enclosed fan–cooled induction electric machine," *IEEE Trans. Ind. Electron.*, vol. 55, no 10, pp. 3517–3524, Oct. 2008.
[21] C. Jungreuthmayer, T. Bäuml, O. Winter, M. Ganchev, H. Kapeller, A. Haumer, and C. Kral, "A detailed heat and fluid flow analysis of an internal permanent magnet synchronous machine by means of computational fluid dynamics," *IEEE Trans. Ind. Electron.*, vol. 59, no 12, pp. 4568–4578, Dec. 2012.
[22] J. Han, W. Li, and Y. Li, "Analysis of three–dimensional complex fluid flow and temperature distribution in the end region of a turbogenerator," *IEEE Trans. Ind. Electron.*, vol. 62, no. 9, pp. 5370–5381, Sep. 2015.
[23] Y. Lu, L. Liu, and D. Zhang, "Simulation and analysis of thermal fields of rotor multislots for nonsalient–pole motor," *IEEE Trans. Ind. Electron.*, vol. 62, no. 12, pp. 7678–7686, Dec. 2015.
[24] R. Camilleri, D. A. Howey, and M. D. McCulloch, "Predicting the temperature and flow distribution in a direct oil–cooled electrical machine with segmented stator," *IEEE Trans. Ind. Electron.*, vol. 63, no. 1, pp. 82–91, Jan. 2016.
[25] H. Si and K. Gärtner, "Meshing piecewise linear complexes by constrained Delaunay tetrahedralizations," *Proc. 14th International Meshing Roundtable*, 2005.
[26] C. Geuzaine and J.–F. Remacle, "Gmsh: a three–dimensional finite element mesh generator with built–in pre– and post–processing facilities," *International Journal for Numerical Methods in Engineering*, vol. 79, no 11, pp. 1309–1331, 2009.
[27] E. M. Tsampouris, M. E. Beniakar, and A. G. Kladas, "Geometry optimization of PMSMs comparing full and fractional pitch winding configurations for aerospace actuation applications," *IEEE Trans. Magn.*, vol. 48, no. 2, pp. 943–946, Feb. 2012.
[28] B. Zhang, R. Qu, W. Xu, J. Wang, and Y. Chen, "Thermal model of totally enclosed water–cooled permanent magnet synchronous machines for electric vehicle applications," in *Proc. ICEM*, 2014, pp. 2205–2211.
[29] A. Nollau and D. Gerling, "Novel cooling methods using flux–barriers," in *Proc. ICEM*, 2014, pp. 1328–1333.
[30] T. Kefalas, G. Kalokiris, A. Kladas, and J. Tegopoulos, "Design of skewed mounted permanent magnet synchronous generators based on 2D and 3D finite element techniques," *Journal of Materials Processing Technology*, vol. 161, pp. 288–293, 2005.
[31] G. D. Kalokiris, T. D. Kefalas, A. G. Kladas, and J. A. Tegopoulos, "Special air–gap element for 2–D FEM analysis of electrical machines accounting for rotor skew," *IEEE Trans. Magn.*, vol. 41, no. 5, pp. 2020–2023, May 2005.
[32] A. S. Thomas, Z. Q. Zhu, and G. J. Li, "Thermal modelling of switched flux permanent magnet machines," in *Proc. ICEM*, 2014, pp. 2212–2217.
[33] X. Wu, R. Wrobel, P. H. Mellor, and C. Zhang, "A computationally efficient PM power loss mapping for brushless AC PM machines with surface–mounted PM rotor construction," *IEEE Trans. Ind. Electron.*, vol. 62, no. 12, pp. 7391–7401, Dec. 2015.

VIII. BIOGRAPHIES

Themistoklis D. Kefalas (M'09) was born in Greece in 1977. He received the Electrical Engineering Educator degree from the School of Pedagogical and Technological Education, Athens, Greece, in 1999 and the Diploma and the Ph.D. degree in electrical engineering from the National Technical University of Athens, Athens, Greece, in 2005 and 2008, respectively.

Since 2010, he has been an Adjunct Assistant Professor with the School of Pedagogical and Technological Education. Since 2008, he has been an Adjunct Lecturer and Research Associate with the School of Electrical and Computer Engineering, National Technical University of Athens. His research interests include electric machine and transformer design, modeling, and optimization.

Dr. Kefalas is a member of the Technical Chamber of Greece.

Antonios G. Kladas (S'80–A'99–M'02–SM'10) was born in Greece in 1959. He received the Diploma in electrical engineering from the Aristotle University of Thessaloniki, Thessaloniki, Greece, in 1982 and the D.E.A. and Ph.D. degrees from Pierre and Marie Curie University (Paris 6), Paris, France, in 1983 and 1987, respectively.

From 1984 to 1989, he was an Associate Assistant with Pierre and Marie Curie University. From 1991 to 1996, he was with Public Power Corporation S.A., Athens, Greece, where he was engaged in the System Studies Department. Since 1996, he has been with the School of Electrical and Computer Engineering, National Technical University of Athens, Athens, Greece, where he is currently a Professor. His research interests include transformer and electric machine modeling and design, as well as the analysis of generating units by renewable energy sources and industrial drives.

Dr. Kladas is a member of the Technical Chamber of Greece.